MODELLING & SIMULATION OF THE DYNAMIC BEHAVIOUR OF A PUMP/PIPELINE SYSTEM.

Dr.ir. S.A. Miedema[1]

ABSTRACT.

Slurry transport is used in dredging and mining to transport solid/liquid mixtures over a long distance. In slurry transport very often multiple pumps are used. To describe the processes involved, very often a steady state approach is used. A steady state process however requires a constant density and solids properties in the system and thus at the suction mouth. In practice it is known, that the solids properties and the density change with respect to time. As a result, the pump discharge pressure and vacuum will change with respect to time and the pipeline resistance will change with respect to time and place. A change of the discharge pressure will result in a change of the torque on the axis of the pump drive on one hand and in a change of the flow velocity on the other hand. The mixture in the pipeline has to accelerate or decelerate. Since centrifugal pumps respond to a change in density and solids properties at the moment the mixture passes the pump, while the pipeline resistance is determined by the contents of the pipeline as a whole, this forms a complex dynamic system.

In this paper an attempt is made to model this dynamic system and give boundary conditions for flow control. From the physical process description a mathematical formulation/algorithm is derived. The results of simulations with and without flow control are shown.

INTRODUCTION.

A multi pump/pipeline system consists of components with different dynamic behaviour. To model such a system, one should start with simple mathematical descriptions of the sub-systems, to be able to determine the sensitivity of the behaviour of the system to changes in one of the sub-systems. The following sub-systems can be distinguished:

- The pump drive
- The centrifugal pump
- The sand/water slurry in the pipeline
- Flow control (if used)

The system is limited by cavitation at the entrance of each pump on one hand and by sedimentation of the solids resulting in plugging of the pipeline on the other hand. Cavitation will occur at high line velocities and/or at high solids concentrations in the suction pipe of the pump considered. Sedimentation will occur at line velocities below the so called critical velocity. The critical velocity depends on the grain distribution and

[1]Associate Professor, Chair of Dredging Technology, Delft University of Technology

on the solids concentration. In between these two limitations a stable transportation process is required. A steady state process is possible only if the solids properties and the solids concentration are constant in time. In practice however this will never be the case. Solids properties such as the grain size distribution will change as a function of time and place as will the solids concentration. The resistance of the slurry flow depends on the solids properties and concentration. If the total resistance of the slurry flow in a long pipeline is considered, changes of the solids properties and concentration at the suction mouth will result in slow changes of the total resistance, since only a small part of the pipeline is filled with the new slurry while most of the pipeline remains filled with the slurry that was already there, except from the slurry that has left the pipeline at the end. If the relatively short suction line is considered, this results in a much faster change of the vacuum at the inlet of the first pump.
The total head of a pump however, responds immediately to changes of the solids properties and concentration. If a sudden increase of the concentration is assumed, the total head of a pump will increase almost proportionally with the concentration. This will result in a higher flow velocity, but, because of the inertia of the slurry mass in the pipeline, the slurry mass will have to accelerate, so the flow velocity responds slowly on changes of the total head. The increase of the total head also causes an increase of the torque and power of the pump drive, resulting in a decrease of the pump drive revolutions and thus of the total head. Because of the inertia of pump and pump drive, there will not be an immediate response.
It is obvious that there is an interaction between all the different sub-systems. These interactions can be ranged from very slow to immediate. To be able to model the system, first the characteristic behaviour of the sub-systems should be known.

THE PUMP DRIVE.

Pump drives used in dredging are diesel direct drives, diesel/electric drives and diesel/hydraulic drives. In this paper the diesel direct drive, as the most common arrangement, is considered.
At nominal operating speed, the maximum load coincides with the nominal full torque point. If the torque is less then the nominal full torque, the engine speed usually rises slightly as the torque decreases. This is the result of the control of the speed by the governor. The extent of this depends upon the type of governor fitted.
If the engine load increases above the full torque point, the speed decreases and the engine operates in the full fuel range. With most diesel engines the torque will increase slightly as the speed decreases, because of a slightly increasing efficiency of the fuel pumps. When the load increases further, insufficient air is available to produce complete combustion and the engine stalls. The torque drops rapidly and heavily polluted gasses are emitted. The smoke limit has been reached. The speed range between the full torque point and the smoke limit is often referred to as the constant torque range.

The torque/speed characteristic of the diesel engine can thus be approximated by a constant full torque upon the nominal operating speed, followed by a quick decrease of the torque in the governor range.
This characteristic however is valid for a steady state process of the diesel engine. When the speed of the diesel changes, the load will change, but also the inertia effects of the diesel have to be taken into account. The equation of motion of the diesel engine, gear box and centrifugal pump combination, reduced to the axis of the centrifugal pump, is:

$$\left(\mathbf{I}_{\mathbf{d.e.}} + \mathbf{I}_{\mathbf{g.b.}} + \mathbf{I}_{\mathbf{c.p.}}\right) \cdot \ddot{\varphi} = \mathbf{T}_{\mathbf{d.e.}} - \mathbf{T}_{\mathbf{h.t.}} \tag{1}$$

In a steady state situation, the torque delivered by the diesel engine $\mathbf{T}_{\mathbf{d.e.}}$ equals the torque required by the hydraulic transport $\mathbf{T}_{\mathbf{h.t.}}$, so the angular acceleration of the diesel is zero. If $\mathbf{T}_{\mathbf{d.e.}}$ is greater then $\mathbf{T}_{\mathbf{h.t.}}$, the revolutions will increase, If $\mathbf{T}_{\mathbf{d.e.}}$ is smaller then $\mathbf{T}_{\mathbf{h.t.}}$, the revolutions will decrease. If the difference between these two torque's is approximated to be proportional with the difference between the actual angular velocity and the nominal operating angular velocity:

$$\mathbf{T}_{\mathbf{d.e.}} - \mathbf{T}_{\mathbf{h.t.}} = \mathbf{K}_{\mathbf{p}} \cdot \left(\dot{\varphi}_{\mathbf{s.p.}} - \dot{\varphi}\right) \tag{2}$$

The linear differential equation can be written as:

$$\left(\mathbf{I}_{\mathbf{d.e.}} + \mathbf{I}_{\mathbf{g.b.}} + \mathbf{I}_{\mathbf{c.p.}}\right) \cdot \ddot{\varphi} = \mathbf{K}_{\mathbf{p}} \cdot \left(\dot{\varphi}_{\mathbf{s.p.}} - \dot{\varphi}\right) \tag{3}$$

With: $\left(\mathbf{I}_{\mathbf{d.e.}} + \mathbf{I}_{\mathbf{g.b.}} + \mathbf{I}_{\mathbf{c.p.}}\right) = \mathbf{I}_{\mathbf{t}}$ and $\tau_{\mathbf{d.e.}} = \dfrac{\mathbf{K}_{\mathbf{p}}}{\mathbf{I}_{\mathbf{t}}}$

The solution of this first order system is:

$$\dot{\varphi} = \dot{\varphi}_{\mathbf{0}} + \left(\dot{\varphi}_{\mathbf{s.p.}} - \dot{\varphi}_{\mathbf{0}}\right) \cdot \left(\mathbf{1} - \mathbf{e}^{-\mathbf{t}/\tau_{\mathbf{d.e.}}}\right) \tag{4}$$

In which $\dot{\varphi}_{\mathbf{0}}$ is the angular velocity at an arbitrary time, defined as **t=0**. Using time domain calculations with a time step $\mathbf{\Delta t}$, the angular velocity at time step **n** can now be written as a function of the angular velocity at time step **n-1** and the set point angular velocity $\dot{\varphi}_{\mathbf{s.p.}}$ according to:

$$\dot{\varphi}_{\mathbf{n}} = \dot{\varphi}_{\mathbf{n-1}} + \left(\dot{\varphi}_{\mathbf{s.p.}} - \dot{\varphi}_{\mathbf{n-1}}\right) \cdot \left(\mathbf{1} - \mathbf{e}^{-\mathbf{\Delta t}/\tau_{\mathbf{d.e.}}}\right) \tag{5}$$

THE CENTRIFUGAL PUMP.

The behaviour of centrifugal pumps can be described with the Euler impulse moment equation:

$$\Delta p_E = \rho_f \cdot u_o \cdot \left(u_o - \frac{Q \cdot \cot(\beta_o)}{2 \cdot \pi \cdot r_o} \right) - \rho_f \cdot u_i \cdot \left(u_i - \frac{Q \cdot \cot(\beta_i)}{2 \cdot \pi \cdot r_i} \right) \tag{6}$$

For a known pump this can be simplified to:

$$\Delta p_E = \rho_f \cdot \left(C_1 - C_2 \cdot Q \right) \tag{7}$$

Because of incongruity of impeller blades and flow, the finite number of blades, the blade thickness and the internal friction of the fluid, the Euler pressure Δp_E has to be corrected with a factor **k**, with a value of about 0.8. This factor however does not influence the efficiency. The resulting equation has to be corrected for losses from frictional contact with the walls and deflection and diversion in the pump and a correction for inlet and impact losses. The pressure reduction for the frictional losses is:

$$\Delta p_{h.f.} = C_3 \cdot \rho_f \cdot Q^2 \tag{8}$$

For a given design flow Q_d the impact losses can be described with:

$$\Delta p_{h.i.} = C_4 \cdot \rho_f \cdot \left(Q_d - Q \right)^2 \tag{9}$$

The total head of the pump as a function of the flow is now:

$$\Delta p_p = k \cdot \Delta p_E - \Delta p_{h.f.} - \Delta p_{h.i.} = \rho_f \cdot \left(k \cdot \left(C_1 - C_2 \cdot Q \right) - C_3 \cdot Q^2 - C_4 \cdot \left(Q_d - Q \right)^2 \right) \tag{10}$$

This is a second degree polynomial in **Q**. The fluid density ρ_f in the pump can be either the density of a homogeneous fluid (for water ρ_w) or the density of a mixture ρ_m passing the pump.
The total efficiency of the pump can be determined by dividing the power that is added to the flow $P_{fl} = \Delta p_p \cdot Q$ by the power that is output of the diesel engine $P_{d.e.} = k \cdot \Delta p_E \cdot Q + P_{d.f.}$ (in which $P_{d.f.}$ is the power required for the frictional losses in the gear box, the pump bearings, etc.), this gives:

$$\eta_p = \frac{(k \cdot \Delta p_E - \Delta p_{h.f.} - \Delta p_{h.i.}) \cdot Q}{k \cdot \Delta p_E \cdot Q + P_{d.f.}} \qquad (11)$$

For the efficiency curve a third degree polynomial approximation satisfies, while the power and torque curves approximate straight lines. The pump characteristics usually will be measured for a specific impeller diameter and number of revolutions.

In a dynamic system however, the pump revolutions will change. This is on one hand the result of the torque/speed curve of the pump drive, on the other hand of manual or automatic flow control. This means that the pump characteristics should also be known at different pump speeds.

The so-called affinity laws describe the influence of a different impeller diameter or revolutions on the pump head, flow and efficiency:

$$\frac{p_1}{p_2} = \frac{n_1^2}{n_2^2} = \frac{D_1^2}{D_2^2}, \qquad \frac{Q_1}{Q_2} = \frac{n_1}{n_2} = \frac{D_1^2}{D_2^2}, \qquad \eta_1 = \eta_2 \qquad (12)$$

The efficiency does not change, but the value of the flow on the horizontal axis is shifted. The affinity laws for the power and the torque can easily be derived from these equations.

$$\frac{P_1}{P_2} = \frac{p_1 \cdot Q_1 \cdot \eta_2}{p_2 \cdot Q_2 \cdot \eta_1} = \frac{n_1^3}{n_2^3} = \frac{D_1^4}{D_2^4}, \qquad \frac{T_1}{T_2} = \frac{P_1 \cdot n_2}{P_2 \cdot n_1} = \frac{p_1 \cdot Q_1 \cdot \eta_2 \cdot n_2}{p_2 \cdot Q_2 \cdot \eta_1 \cdot n_1} = \frac{n_1^2}{n_2^2} = \frac{D_1^4}{D_2^4} \qquad (13)$$

If a ratio for the revolutions $\varepsilon_n = \frac{n}{n_m}$ and a ratio for the diameter $\varepsilon_D = \frac{D}{D_m}$ are given, the head and efficiency curves at a speed **n** and an impeller diameter **D** can be determined by:

$$Q = Q_m \cdot \varepsilon_n^1 \cdot \varepsilon_D^2 \qquad (14)$$

$$\Delta p_p = \alpha_0 \cdot Q^0 \cdot \varepsilon_n^2 \cdot \varepsilon_D^2 + \alpha_1 \cdot Q^1 \cdot \varepsilon_n^1 \cdot \varepsilon_D^0 + \alpha_2 \cdot Q^2 \cdot \varepsilon_n^0 \cdot \varepsilon_D^{-2} \qquad (15)$$

$$\eta_p = \beta_0 \cdot Q^0 \cdot \varepsilon_n^0 \cdot \varepsilon_D^0 + \beta_1 \cdot Q^1 \cdot \varepsilon_n^{-1} \cdot \varepsilon_D^{-2} + \beta_2 \cdot Q^2 \cdot \varepsilon_n^{-2} \cdot \varepsilon_D^{-4} + \beta_3 \cdot Q^3 \cdot \varepsilon_n^{-3} \cdot \varepsilon_D^{-6} \qquad (16)$$

In which n_m, D_m and Q_m are the revolutions, impeller diameter and flow used in the measurements of the head and efficiency curves.

Based on this theory, the characteristics of two pumps used in the case study in this paper, are given in figures 1 and 2. Both pumps are limited by the constant torque behaviour of the corresponding diesel engine in the full fuel range.

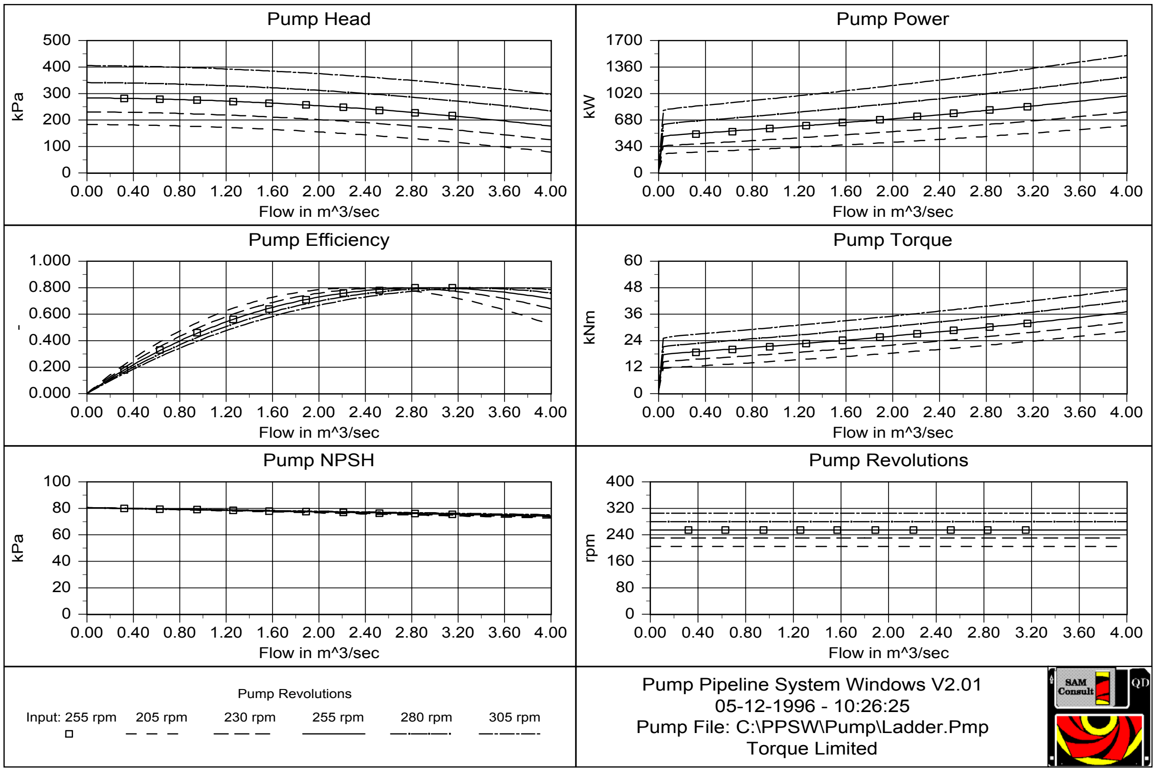

Fig. 1: The characteristics of the ladder pump.

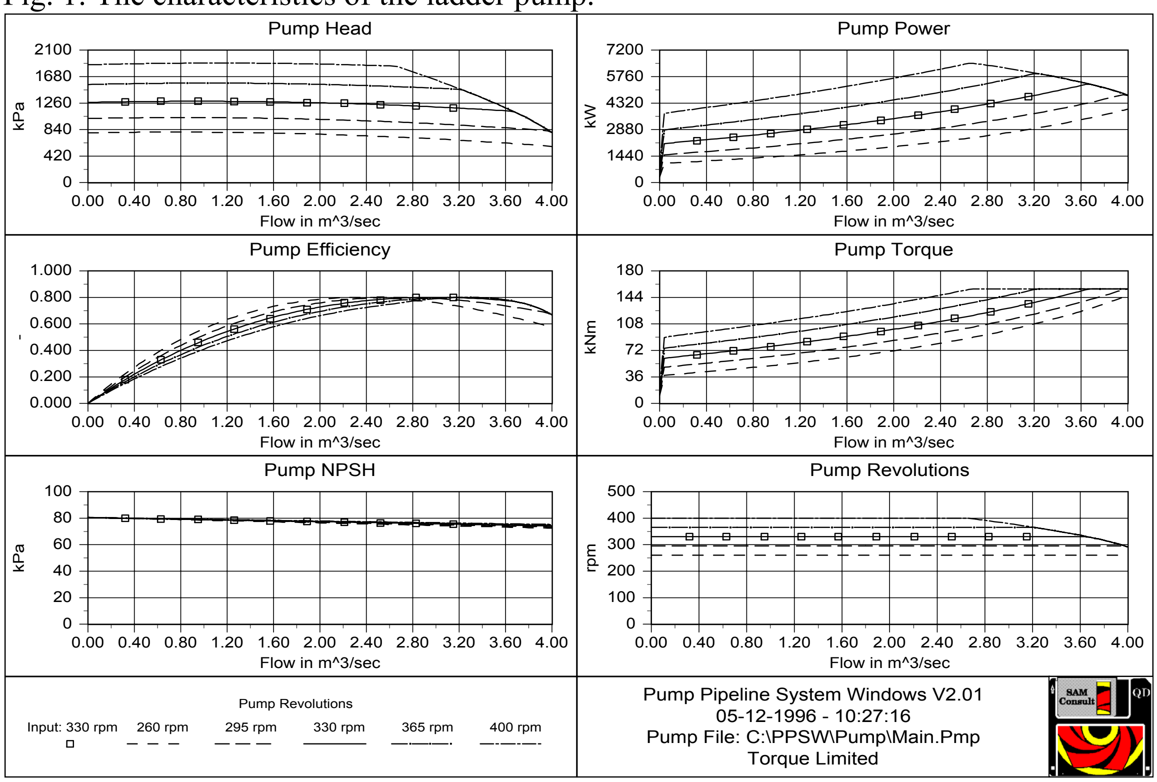

Fig. 2: The characteristics of the main pump and the booster pump.

Figures 1 and 2 give the pump characteristics for clear water. If a mixture is pumped however, the pump head increases because of the mixture density as has been pointed out when discussing equation 10 and the pump efficiency decreases because a heterogeneous mixture is flowing through the pump. The decrease of the efficiency depends upon the average grain diameter, the impeller diameter and the solids concentration and can be determined with (according to Stepanoff):

$$\eta_{m} = \left(1 - C_{t} \cdot \left(0.466 + 0.4 \cdot \mathrm{Log10}\left(d_{50}\right)\right) / D\right) \tag{17}$$

PRESSURE LOSSES WITH HOMOGENEOUS WATER FLOW.

When clear water flows through the pipeline, the pressure loss can be determined with the well known Darcy-Weisbach equation:

$$\Delta p_{w} = \lambda \cdot \frac{L}{D} \cdot \frac{1}{2} \cdot \rho_{w} \cdot c^{2} \tag{18}$$

The value of the friction factor λ depends on the Reynolds number:

$$Re = \frac{c \cdot D}{\nu} \tag{19}$$

For laminar flow (Re<2320) the value of λ can be determined according to Poiseuille:

$$\lambda = \frac{64}{Re} \tag{20}$$

For turbulent flow (Re>2320) the value of λ depends not only on the Reynolds number but also on the relative roughness of the pipe **ε/D**. A general implicit equation for λ is the Colebrook-White equation:

$$\lambda = \frac{1}{\left(2 \cdot \mathrm{Log}\left(\frac{2.51}{Re \cdot \sqrt{\lambda}} + \frac{0.27 \cdot \varepsilon}{D}\right)\right)^{2}} \tag{21}$$

For very smooth pipes the value of the relative roughness **ε/D** is almost zero, resulting in the Prandl & von Karman equation:

$$\lambda = \frac{1}{\left(2 \cdot \mathrm{Log}\left(\frac{2.51}{\mathrm{Re} \cdot \sqrt{\lambda}}\right)\right)^2} \tag{22}$$

At very high Reynolds numbers the value of **2.51/(Re·√λ)** is almost zero, resulting in the Nikuradse equation:

$$\lambda = \frac{1}{\left(2 \cdot \mathrm{Log}\left(\frac{0.27 \cdot \varepsilon}{D}\right)\right)^2} \tag{23}$$

Because equations 21 and 22 are implicit, for smooth pipes approximation equations can be used. For a Reynolds number between 2320 and 10^5 the Blasius equation gives a good approximation:

$$\lambda = 0.3164 + \left(\frac{1}{\mathrm{Re}}\right)^{0.25} \tag{24}$$

For a Reynolds number in the range of 10^5 to 10^8 the Nikuradse equation gives a good approximation:

$$\lambda = 0.0032 + \frac{0.221}{\mathrm{Re}^{0.237}} \tag{25}$$

PRESSURE LOSSES WITH HETEROGENEOUS FLOW.

For the determination of the pressure losses of a heterogeneous flow many theories are available, like Durand/Condolios/Gibert, Fuhrboter, Jufin/Lopatin and Wilson. In this paper the Durand/Condolios/Gibert theory will be used, further referred to as the Durand theory. Durand assumes that the clear water resistance in a pipeline should be multiplied by a factor depending on the line speed, the grain size distribution and the concentration, according to:

$$\Delta p_m = \Delta p_w \cdot \left(1 + \Phi \cdot C_t\right) + \sum_1^n \xi_n \cdot \tfrac{1}{2} \cdot \rho_m \cdot c^2 + \rho_m \cdot g \cdot H_g + \rho_m \cdot L \cdot \dot{c} \tag{26}$$

In which:

$$\Phi = 180 \cdot \left(\frac{c^2}{g \cdot D} \cdot \sqrt{C_x}\right)^{-3/2} \tag{27}$$

and:

$$\mathbf{C_x = \frac{g \cdot d}{v^2}} \tag{28}$$

The second term in the right hand side gives the resistance of all bendings, valves, etc. The third term gives the resistance of the geodetic height and the fourth term the inertial resistance. Since $\mathbf{Fr_{fl} = \frac{c}{\sqrt{g \cdot D_p}}}$ is the Froude number for the flow in the pipeline and $\mathbf{Fr_{gr} = \frac{v}{\sqrt{g \cdot d}}}$ is the Froude number for the settling process of a grain, equation 27 can also be written as:

$$\mathbf{\Phi = 176 \cdot Fr_{fl}^{-3} \cdot Fr_{gr}^{1.5}} \tag{29}$$

In normal sands, there is not only one graindiameter, but a grain size distribution has to be considered. The Froude number for a grain size distribution can be determined by integrating the Froude number as a function of the probability according to:

$$\mathbf{Fr_{gr} = \frac{1}{\int_0^1 \frac{\sqrt{g \cdot d}}{v} dp}} \tag{30}$$

When the flow decreases, there will be a moment where sedimentation of the grains starts to occur. The corresponding line speed is called the critical velocity. Although in literature researchers do not agree on the formulation of the critical velocity, the value of the critical velocity is often derived by differentiating equation 26 with respect to the line speed **c** and taking the value of **c** where the derivative equals zero. This gives:

$$\mathbf{c_{cr} = \sqrt{\frac{g \cdot D_p \cdot \left(90 \cdot C_t\right)^{2/3}}{\sqrt{C_x}}}} \tag{31}$$

At line speeds less then the critical velocity sedimentation occurs and part of the cross-section of the pipe is filled with sand, resulting in a higher flow velocity above the sediment. Durand assumes an equilibrium between sedimentation and scour, resulting in a Froude number equal to the Froude number at the critical velocity.

$$\mathbf{Fr_{cr}} = \frac{\mathbf{c_{cr}}}{\sqrt{\mathbf{g \cdot D_p}}} = \sqrt{\frac{\left(\mathbf{90 \cdot C_t}\right)^{2/3}}{\sqrt{\mathbf{C_x}}}} \tag{32}$$

By using the hydraulic diameter concept, at lines speeds less then the critical velocity, the resistance can be determined.

THE SETTLING VELOCITY OF GRAINS.

To be able to determine the Froude number for a grain size distribution according to equation 30, the settling velocity of the grains as a function of the grain diameter should be known. The settling velocity of grains depends on the grain size, shape and specific density. It also depends on the density and the viscosity of the fluid the grains are settling in, it also depends upon whether the settling process is laminar or turbulent. In general, the settling velocity **v** can be determined with the following equation:

$$\mathbf{v} = \sqrt{\frac{\mathbf{4 \cdot g \cdot \left(\rho_q - \rho_w\right) \cdot d \cdot \psi}}{\mathbf{3 \cdot \rho_w \cdot C_d}}} \tag{33}$$

The Reynolds number of the settling process determines whether the process is laminar or turbulent. The Reynolds number can be determined by:

$$\mathbf{Re} = \frac{\mathbf{v \cdot d}}{\nu} \tag{34}$$

The drag coefficient $\mathbf{C_d}$ depends upon the Reynolds number according to:

$$\mathbf{Re < 1} \qquad \Rightarrow \qquad \mathbf{C_d} = \frac{\mathbf{24}}{\mathbf{Re}} \tag{35}$$

$$\mathbf{1 < Re < 2000} \qquad \Rightarrow \qquad \mathbf{C_d} = \frac{\mathbf{24}}{\mathbf{Re}} + \frac{\mathbf{3}}{\sqrt{\mathbf{Re}}} + \mathbf{0.34} \tag{36}$$

$$\mathbf{Re > 2000} \qquad \Rightarrow \qquad \mathbf{C_d = 0.4} \tag{37}$$

Stokes, Budryck and Rittinger used these drag coefficients to calculate settling velocities for laminar settling (Stokes), a transition zone (Budryck) and turbulent settling (Rittinger) of sand grains. This gives the following equations for the settling velocity:

Laminar flow, **d<0.1 mm**, according to Stokes.

$$\mathbf{v = 424 \cdot \left(\rho_q - \rho_w\right) \cdot d^2} \tag{38}$$

Transition zone, **d>0.1 mm and d<1 mm**, according to Budryck.

$$\mathbf{v = 8.925 \cdot \frac{\left(\sqrt{\left(1 + 95 \cdot \left(\rho_q - \rho_w\right) \cdot d^3\right)} - 1\right)}{d}} \tag{39}$$

Turbulent flow, **d>1**, according to Rittinger.

$$\mathbf{v = 87 \cdot \sqrt{\left(\left(\rho_q - \rho_w\right) \cdot d\right)}} \tag{40}$$

In these equations the grain diameter is in mm and the settling velocity in mm/sec. Since the equations were derived for sand grains, the shape factor for sand grains is used for determining the constants in the equations. The shape factor can be introduced into the equations for the drag coefficient by dividing the drag coefficient by a shape factor ψ. For normal sands this shape factor has a value of 0.7. The viscosity of the water is temperature dependent. If a temperature of 10° is used as a reference, then the viscosity increases by 27% at 0° and it decreases by 30% at 20° centigrade. Since the viscosity influences the Reynolds number, the settling velocity for laminar settling is also influenced by the viscosity. For turbulent settling the drag coefficient does not depend on the Reynolds number, so this settling process is not influenced by the viscosity. Other researchers use slightly different constants in these equations but, these equations suffice to explain the basics of the Durand theory.

The above equations calculate the settling velocities for individual grains. The grain moves downwards and the same volume of water has to move upwards. In a mixture, this means that, when many grains are settling, an average upwards velocity of the water exists. This results in a decrease of the settling velocity, which is often referred to as hindered settling. However, at very low concentrations the settling velocity will increase because the grains settle in each others shadow. Richardson and Zaki determined an equation to calculate the influence of hindered settling for volume concentrations $\mathbf{C_v}$ between 0 and 0.3. The coefficient in this equation is dependent on the Reynolds number. The general equation yields:

$$\mathbf{\frac{v_c}{v} = \left(1 - C_v\right)^{\beta}} \tag{41}$$

The following values for β should be used:

Re<0.2	β=4.65
Re>0.2 and Re<1.0	$\beta=4.35 \cdot Re^{-0.03}$
Re>1.0 and Re<200	$\beta=4.45 \cdot Re^{-0.1}$
Re>200	β=2.39

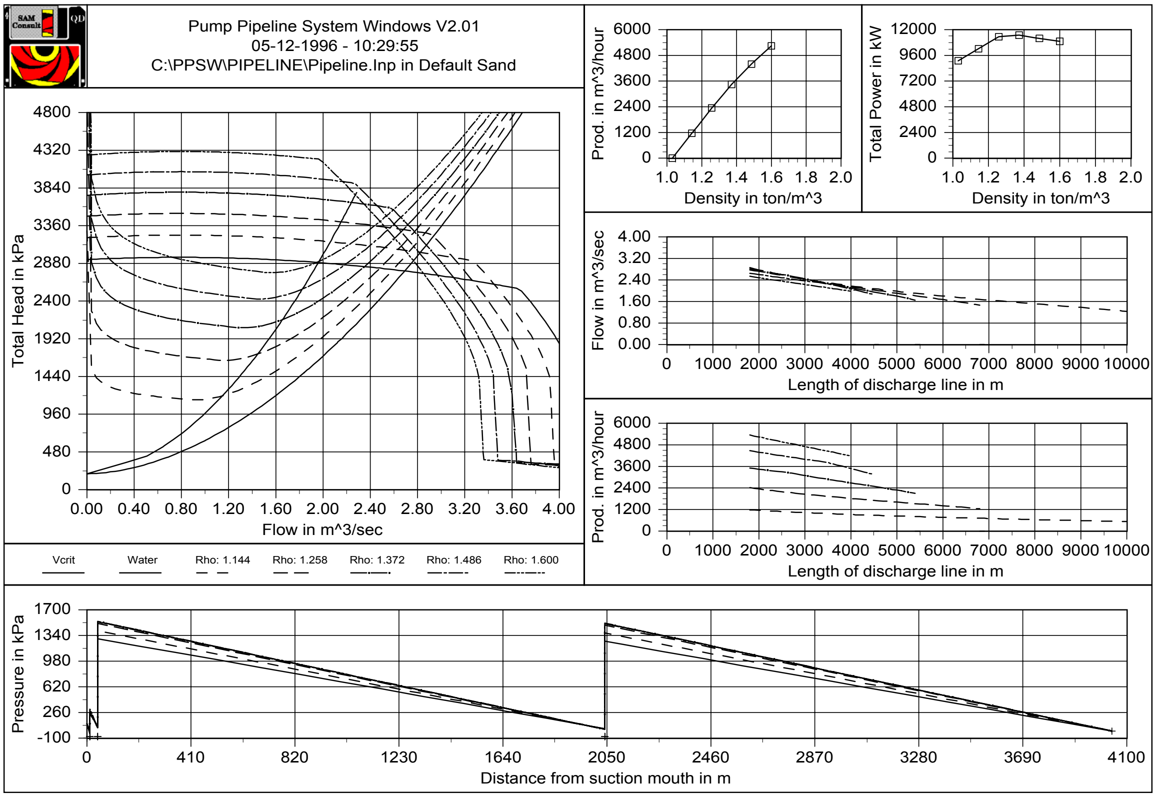

Fig. 3: Characteristics of the pump/pipeline system.

THE PUMP /PIPELINE SYSTEM DESCRIPTION.

In a steady state situation, the revolutions of the pumps are fixed, the line speed is constant and the solids properties and concentration are constant in the pipeline. The working point of the system is the intersection point of the pump head curve and the pipeline resistance curve. The pump curve is a summation of the head curves of each pump according to equation 15. The resistance curve is a summation of the resistances of the pipe segments and the geodetic head according to equation 26. Figure 3 shows this steady state situation for the system used in the case study at 6 densities ranging from clear water upto a density of 1.6 ton/m^3. In reality, the solids properties and concentration are not constant in time at the suction mouth. As a result of this, the solids properties and concentration are not constant as a function of the position in the pipeline. To be able to know these properties as a function of the position in the pipeline, the pipeline must be divided into small segments. These segments move through the pipeline with the line speed. Each time step a new segment is added at the suction mouth, while part of the last segment leaves the pipeline. Because the line speed is not constant, the length of the segment added is not constant, but equals the line speed times the time step. For each segment the resistance is determined, so the resistance as a function of the position in the pipeline is known. This way also the vacuum and the discharge pressure can be determined for each pump. If vacuum results in cavitation of one of the pumps, the pump head is decreased by decreasing the pump density, depending on the time the pump is cavitating. The dynamic calculations are carried out in the time domain, because most of the equations used are non-linear. The time step used is about 1 second, depending on the speed of the PC and the other tasks Windows has to carry out.

CASE STUDY.

The aim of this case study is twofold, first it shows events caused by the dynamic behaviour of the system that cannot be predicted by steady state calculations, second it shows the application of the above theory. A problem in defining a system and a scenario for the simulation is, that the system can consist of an infinite number of pump/pipeline combinations, while there also exists an infinite number of solids property/concentration distributions as a function of time. For this case study, a system is defined consisting of a suction line followed by three pump/pipeline units. The first pump is a ladder pump, with a speed of 200 rpm, an impeller diameter of 1.5 m and 1050 kW on the axis (see fig. 1). The second and the third pump run also at a speed of 200 rpm, have an impeller diameter of 2.4 m and 3250 kW on the axis. The time constants of all three pumps are set to 4 seconds. The time constant of the density meter is set to 10 seconds. The suction line starts at 10 m below water level, has a length of 12 m and a diameter of 0.69 m. The ladder pump is placed 5 m below water level. The main pump and the booster pump are placed 10 m above water level. The pipeline length between ladder and main pump is 30 m, between main pump and booster pump 2000 m, as is the length of the discharge line. The pipe diameters after the ladder pump are 0.61 m. The total simulation lasts about 28 minutes and starts with the pipeline filled with water. After the pumps are activated, a mixture with a density of 1.6 ton/m^3 enters the suction mouth for a period of 2 minutes. A sand is used with a d_{15} of 0.25 mm, a d_{50} of 0.50 mm and a d_{85} of 0.75 mm. This density block wave moves through the system, subsequently passing the three pumps. For the simulation the following scenario is used:

00 minutes	start of simulation
01 minutes	start of ladder pump
04 minutes	start of main pump
07 minutes	start of booster pump
10 minutes	increase mixture density to about 1.6 ton/m^3
12 minutes	decrease mixture density to water density
12 minutes	take sample of density distribution in pipeline
17 minutes	take sample of density distribution in pipeline
22 minutes	take sample of density distribution in pipeline
28 minutes	stop simulation

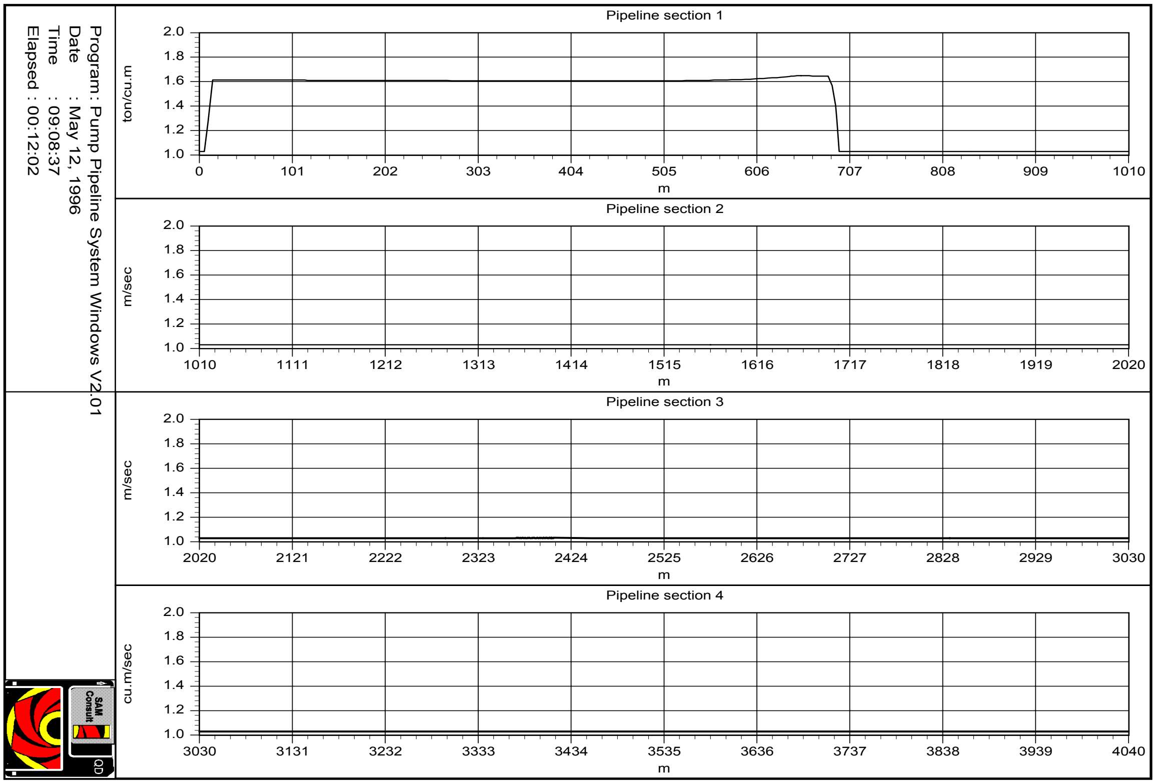

Fig. 4: The density distribution in the pipeline after 12 minutes.

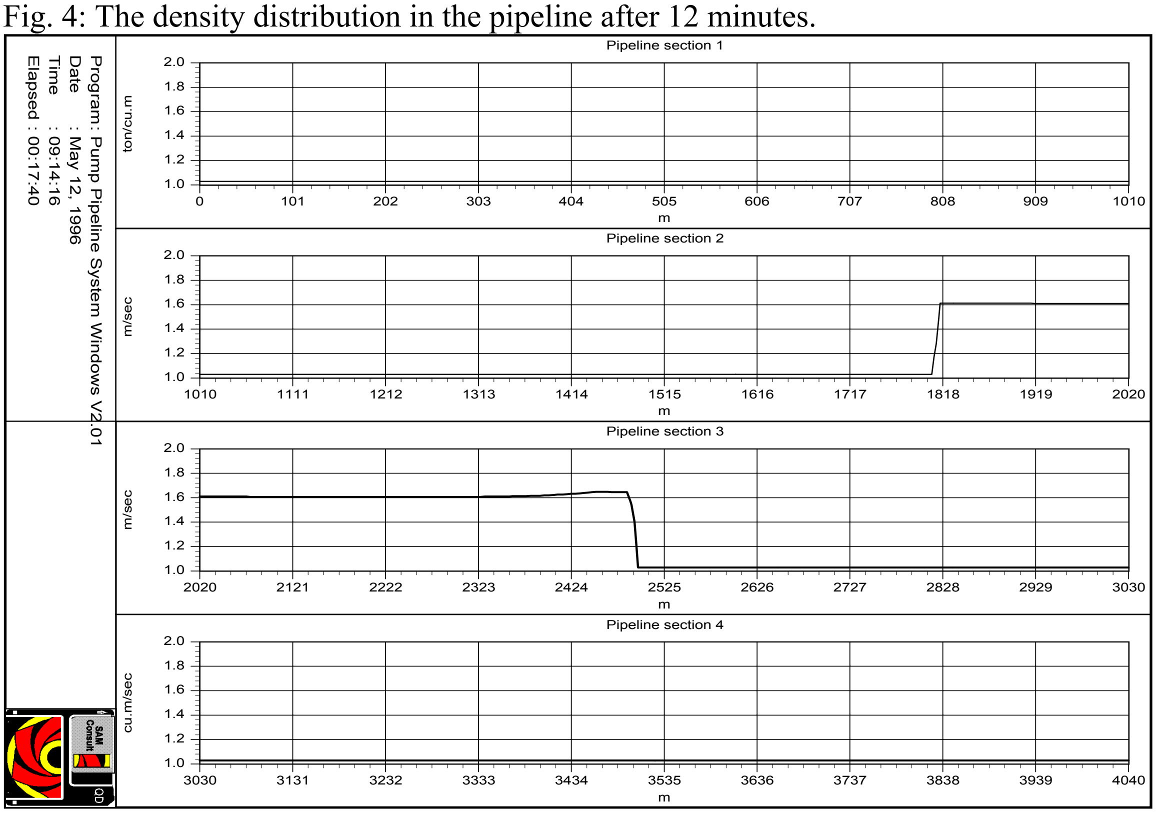

Fig. 5: The density distribution in the pipeline after 17 minutes.

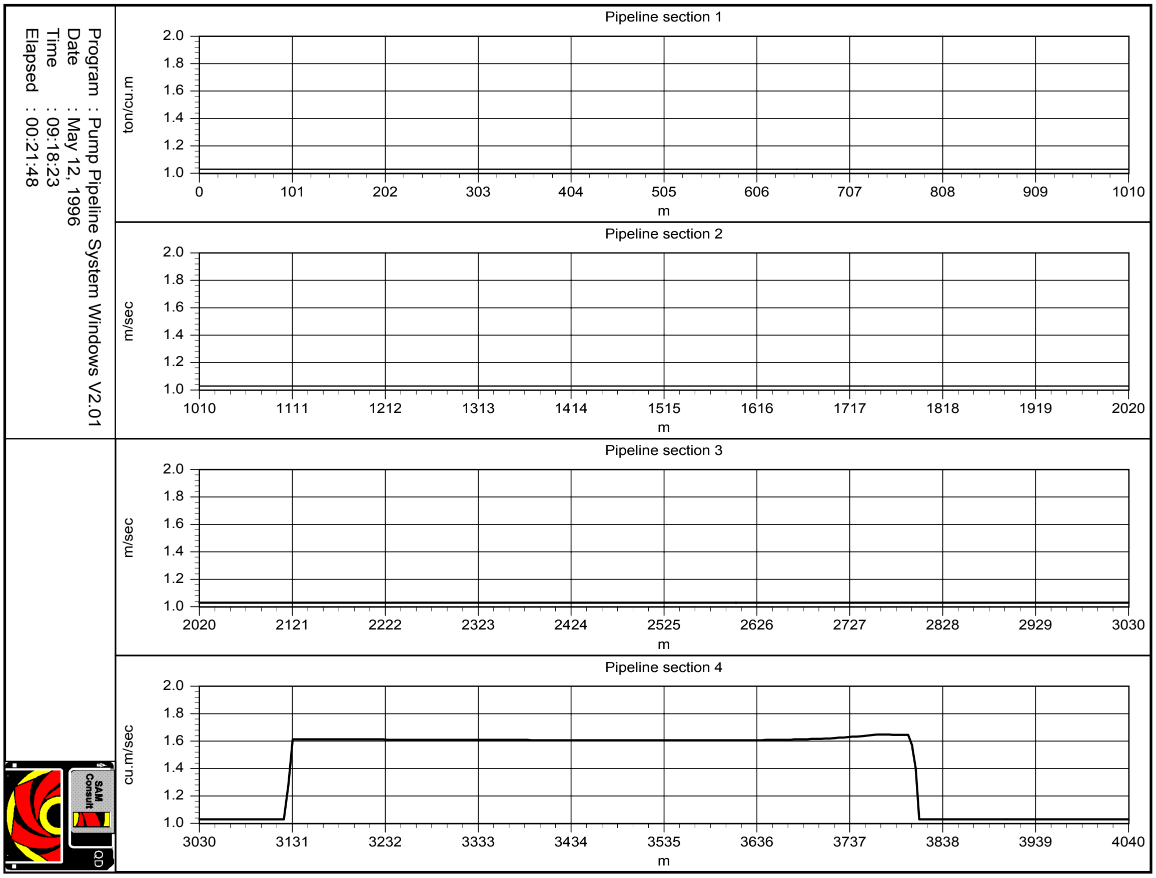

Fig. 6: The density distribution in the pipeline after 22 minutes.

Figures 4, 5 and 6 show the density wave at 12, 17 and 22 minutes of simulation time. At 12 minutes the density wave occupies the suction line, the ladder pump and the main pump and part of the pipeline behind the main pump. At 17 minutes the density wave occupies the last part of the pipeline before the booster pump, the booster pump and the first part of the discharge line after the booster pump. At 22 minutes the density wave occupies the middle part of the discharge line. Figure 7 shows the line speed, the density, the total power consumed and the production as a function of time. The line speed, the density and the production are determined at the inlet of the ladder pump. The density is determined using the mathematical behaviour of a density transducer with a time constant of 10 seconds. Figures 8, 9 and 10 show the pump speed, power, vacuum and discharge pressure of the three pumps as a function of time.

As can be seen in figure 7, the line speed increases slower then the pump speed, due to the inertial effect in the fourth term of equation 26. When the density wave passes the ladder and main pump (from 10 to 13 minutes), the discharge pressure of these pumps increases, resulting in a higher line speed. When the density wave passes the booster pump (from 16 to 19 minutes) the same occurs for the booster pump.

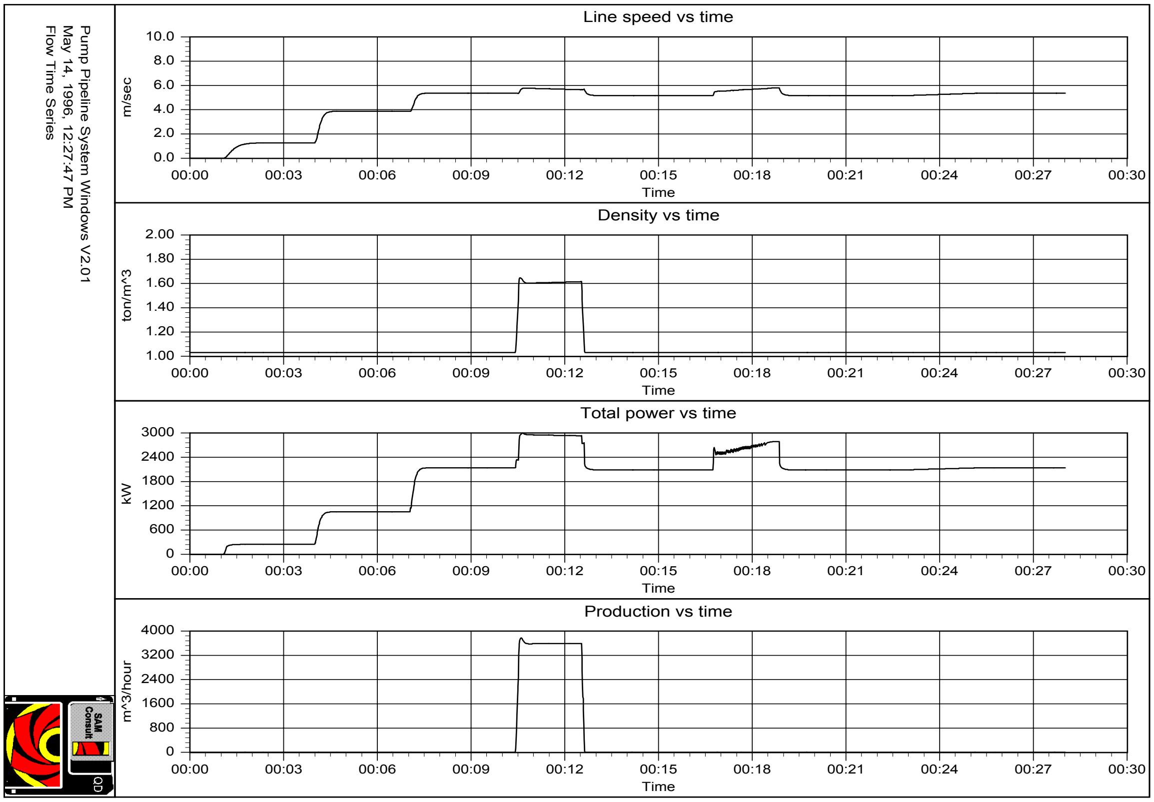

Fig. 7: Line speed, density, total power and situ production as a function of time.

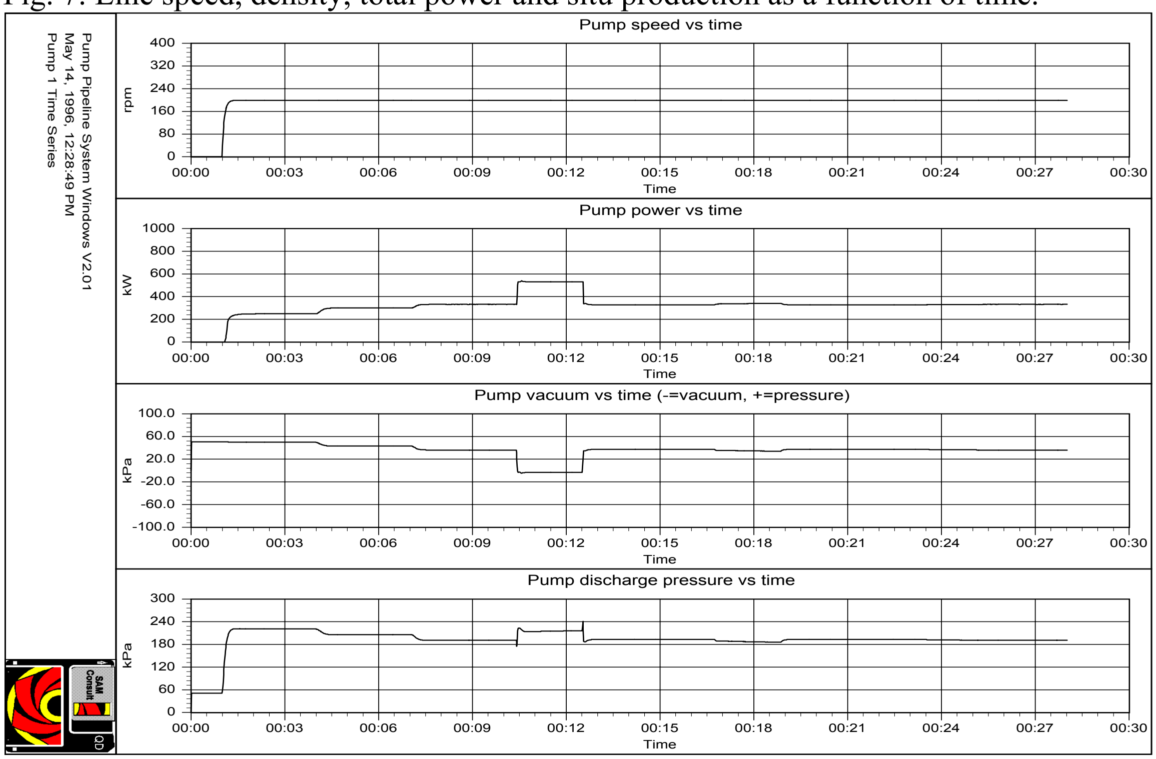

Fig. 8: Speed, power, vacuum and discharge pressure of the ladder pump vs. time.

After about 10 minutes of simulation time, all three pumps are activated and a steady state situation occurs in the system. Then the mixture density at the suction mouth increases from water density to about 1.6 ton/m^3. First the resistance in the suction line increases, resulting in a sudden decrease of the ladder pump vacuum and discharge pressure. When the density wave reaches the ladder pump, the discharge pressure increases, due to the higher density. When after 2 minutes, the density decreases to the water density, first the resistance in the suction line decreases, resulting in an increase of the ladder pump vacuum and discharge pressure, followed by a decrease of the discharge pressure when the clear water reaches the ladder pump (see fig. 7). The distance between the ladder pump and the main pump is 30 m. With an average line speed of 5 m/s, the density wave passes the main pump 6 seconds after passing the ladder pump. The same phenomena as described for the ladder pump, occur 6 seconds later for the main pump (see fig. 9). Due to the increased discharge pressure of ladder and main pump during the density wave, the line speed will also increase (see fig. 7), but because of the inertial effects, this increase and 2 minutes later decrease is not as steep. One could say that there is a time delay between the immidiate response of the discharge pressure of the pumps on changes in the density in the pumps and the response of the line speed on changes in the discharge pressure. At 12 minutes and about 15 seconds, the density wave has left the main pump, but has not yet reached the booster pump. The head of each pump is determined by the density of water, but the line speed is still determined by the head resulting from the mixture and thus to high. The resistance in the pipe between main and booster pump is high because of the mixture, resulting in a decrease of the booster pump vacuum and discharge pressure. As the line speed decreases, the booster pump vacuum and discharge pressure will stay in a semi-steady state situation. When the density wave reaches the booster pump, the total head of the booster pump increases, resulting in an increase of the line speed. This occurs after about 16.5 minutes of simulation time. Since the total head of ladder and main pump does not change, the booster pump vacuum will have to decrease to pull harder on the mixture in the pipeline before the booster pump. This results in the occurence of cavitation of the booster pump, limiting the total head of the booster pump and thus the line speed. The cavitation causes a very instable behaviour of the booster pump as is shown in figure 10. Since the density wave moves from the suction line to the discharge line, the booster pump vacuum and discharge pressure both increase when the density wave moves through the booster pump. After 18.5 minutes the density wave leaves the booster pump. The total head of the booster pump decreases sharply, while the line speed decreases slowly. The fluid in the pipeline before the booster pump pushes and the fluid after the booster pump pulls, resulting in a quick increase of the booster pump vacuum and a decrease in the booster pump discharge pressure. As the line speed decreases, the discharge pressure will increase again. After 23 minutes of simulation time, the density wave starts leaving the pipeline. 2 minutes later the density wave has complete left the system. Because of the decreasing resistance during this time-span, the line speed will increase slightly, resulting in a small decrease of the vacuum and discharge pressure of each pump, while the total

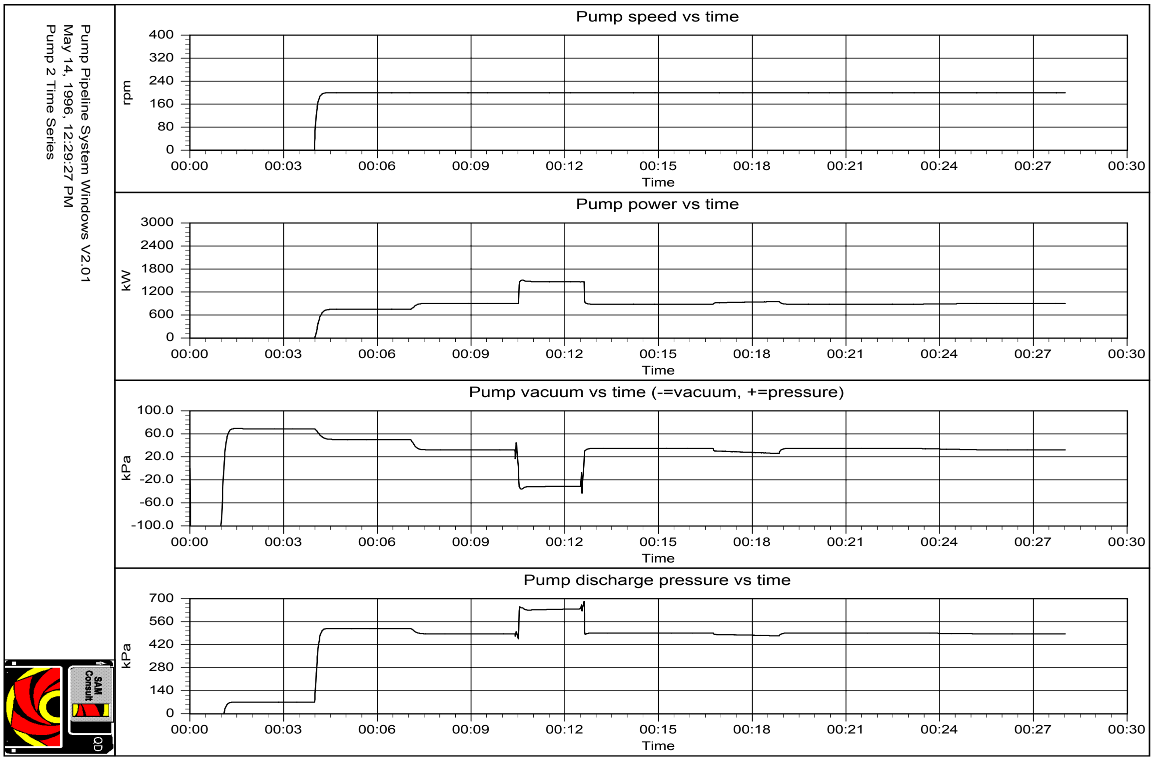

Fig. 9: Speed, power, vacuum and discharge pressure of the main pump vs. time.

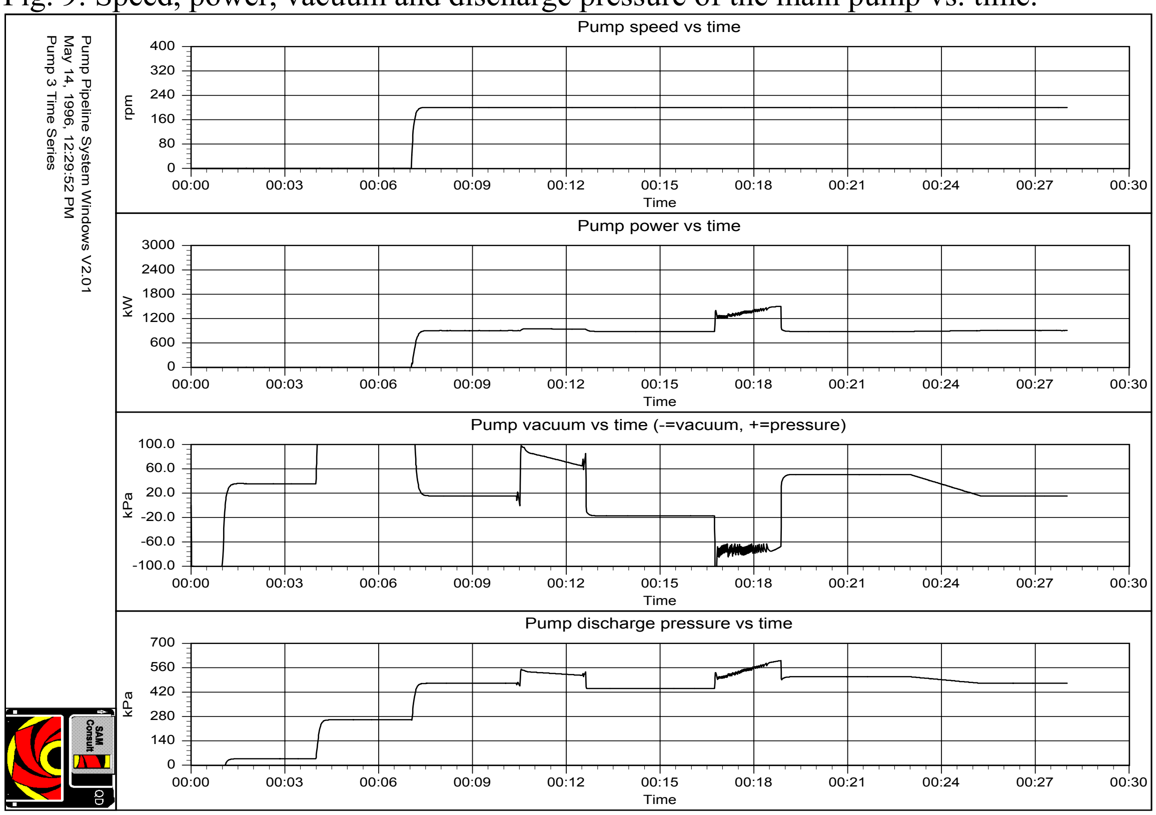

Fig. 10: Speed, power, vacuum and discharge pressure of the booster pump vs. time.

head remains constant. The total power will also increase slightly because of this.
To stabilise the line speed to a specific value, flow control can be used. Flow control adjusts the speed of the last pump, in this case the booster pump. If the line speed is higher then a set point, the booster pump speed is decreased, if the line speed is lower, the booster pump speed is increased. To determine the correct booster pump speed, the total head is considered to be a summation of the heads of all of the pumps in the system. The head of the booster pump is considered to be proportional to the square of the booster pump speed and the total resistance is considered to be proportional to the square of the line speed, this gives:

$$\Delta \mathbf{p}_{\mathbf{l.p.}} + \Delta \mathbf{p}_{\mathbf{m.p.}} + \Delta \mathbf{p}_{\mathbf{b.p.}} = \Delta \mathbf{p}_{\mathbf{l.p.}} + \Delta \mathbf{p}_{\mathbf{m.p.}} + \alpha \cdot \mathbf{n}^2 = \beta \cdot \mathbf{c}^2 \tag{42}$$

When the flow control is active, the heads of the ladder pump and the main pump do not change, so for the set point of the line speed:

$$\Delta \mathbf{p}_{\mathbf{l.p.}} + \Delta \mathbf{p}_{\mathbf{m.p.}} + \Delta \mathbf{p}_{\mathbf{b.p.}} = \Delta \mathbf{p}_{\mathbf{l.p.}} + \Delta \mathbf{p}_{\mathbf{m.p.}} + \alpha \cdot \mathbf{n}_{\mathbf{f.c.}}^2 = \beta \cdot \mathbf{c}_{\mathbf{f.c.}}^2 \tag{43}$$

Assuming that the sum of the heads of ladder and main pump equals the head of the booster pump times a factor γ and dividing equation 43 by equation 42, the following can be derived:

$$\mathbf{n}_{\mathbf{f.c.}} = \mathbf{n} \cdot \sqrt{(\gamma + \mathbf{1}) \cdot \left(\frac{\mathbf{c}_{\mathbf{f.c.}}}{\mathbf{c}}\right)^2 - \gamma} \tag{44}$$

By substituting: $\varepsilon = \left(\frac{\mathbf{c}_{\mathbf{f.c.}} - \mathbf{c}}{\mathbf{c}}\right)$ and using Taylor series approximation, this gives:

$$\mathbf{n}_{\mathbf{f.c.}} = \mathbf{n} + \mathbf{n} \cdot \tfrac{1}{2} \cdot (\gamma + \mathbf{1}) \cdot \varepsilon \cdot (\varepsilon + \mathbf{2}) \tag{45}$$

Equation 45 is used to simulate flow control. The same scenario as above is used, except for the flow control that is activated after 8 minutes of simulation time. The set point for the line speed is set to 5 m/sec. Figures 11 and 12 show the results of this simulation. As can be seen, the line speed changes rapidly when the density wave reaches or leaves one of the pumps. In about 15 seconds the flow control has adjusted the line speed to the set point. Figure 12 shows that the occurrence of cavitation is almost surpressed using the flow control. The booster pump speed tends to slightly oscillate. This is caused by applying several first order systems in series, resulting in a second or third order system. If the factor γ is choosen to high, the system is fast but tends to oscillate. If this factor is to small, the system responds very slow. In the simulation a value of 2 is used.

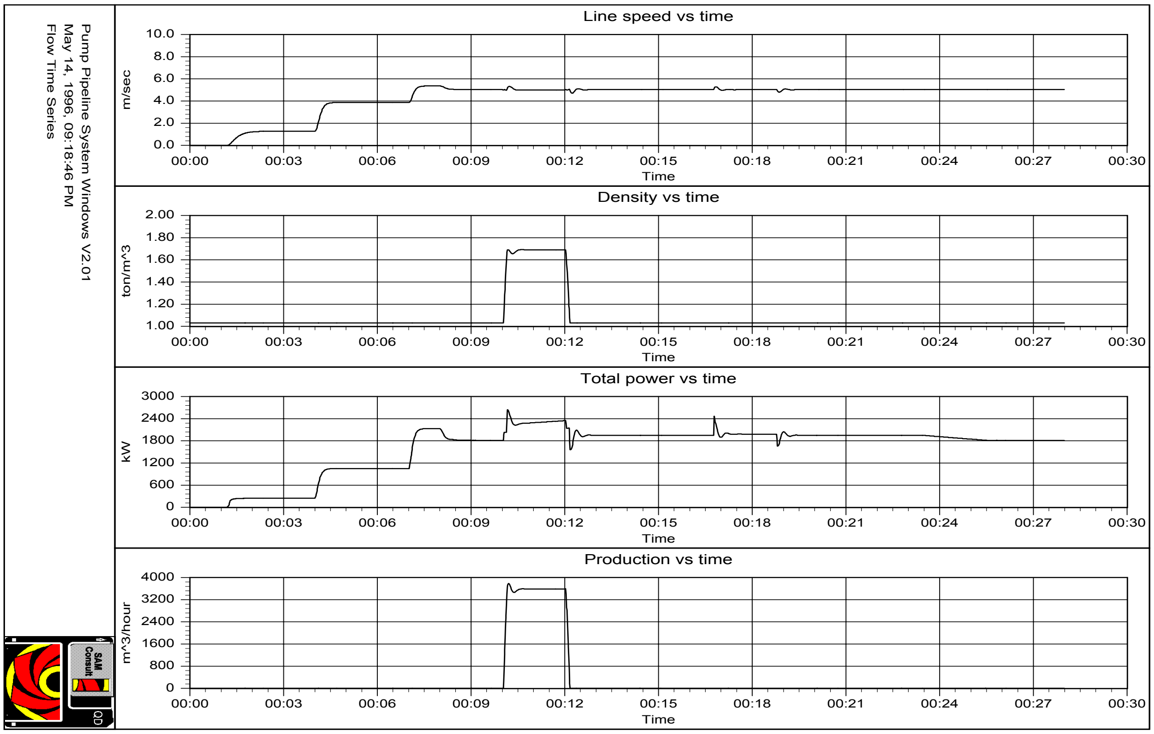

Fig. 11: Line speed, density, total power and situ production as a function of time, with flow control.

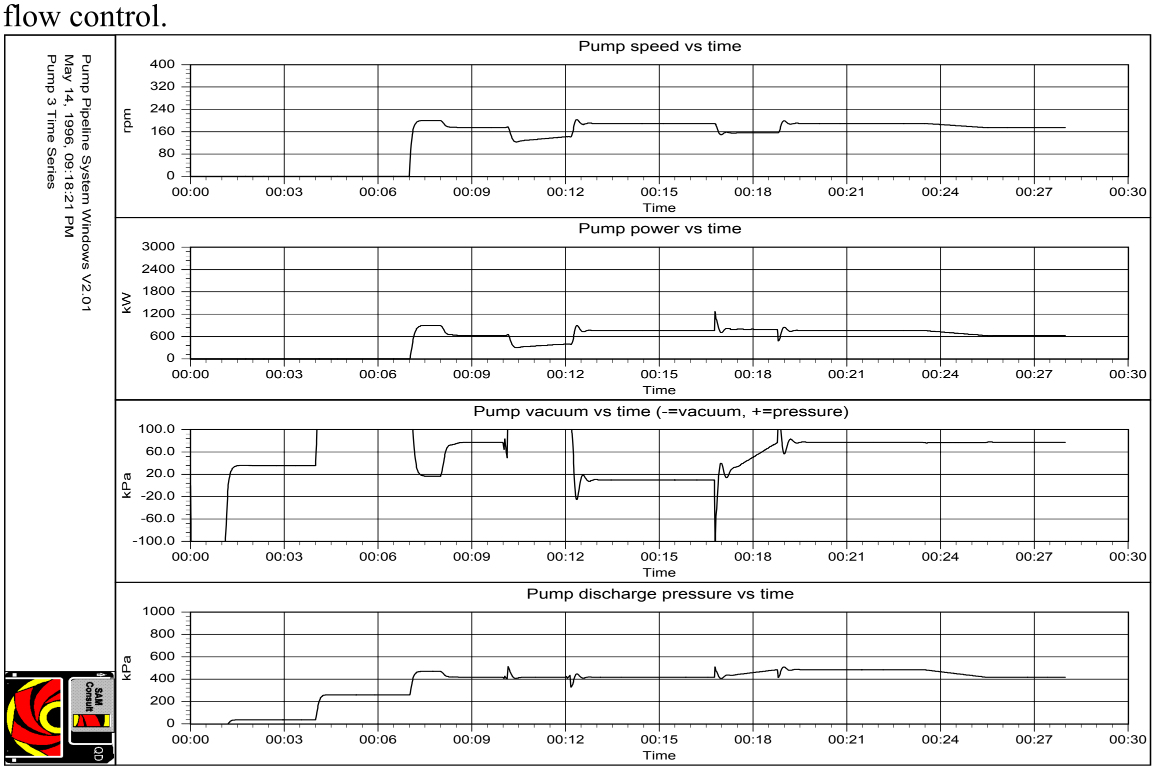

Fig. 12: Speed, power, vacuum and discharge pressure of the booster pump vs. time, with flow control.

CONCLUSIONS AND DISCUSSION.

The behaviour of a multi pump/pipeline system is hard to understand. As mentioned before, an infinite number of system configurations and soil conditions exist. Systems are usually configured, based on steady state calculations, while the dynamic behaviour is ignored. Combining the steady state approach for pipeline resistance with the dynamic behaviour of pumps, pump drives and the second law of Newton, the dynamic behaviour can be simulated. However, a number of assumptions had to be made.

These assumptions are:

There is no longitudinal diffusion in the pipeline.
The pump drive behaves like a constant torque system.
The pipeline resistance is determined using the Durand theory.
The centrifugal pump obeys the affinity laws.

Whether these assumptions are valid will be subject of further research.

The simulations however show the occurrence of phenomena that are known in practice.

One should consider that mathematical modelling is an attempt to describe reality without having any presumption of being reality.

LITERATURE.

Bree, S.E.M. de 1977, "Centrifugal Dredgepumps". IHC Holland 1977.
Gibert, R., "Transport Hydraulique et Refoulement des Mixtures en Conduites".
Huisman, L. 1995, "Sedimentation and Flotation". Lecture Notes, Delft University Of Technology 1973-1995.
Miedema, S.A. 1996, "Pump Pipeline System Windows V2.01". Software, Delft 1996.
Wilson, K.C. & Addie, G.R. & Clift, R. 1992, "Slurry Transport Using Centrifugal Pumps". Elsevier Science Publishers Ltd. 1992.

NOMENCLATURE.

c	Line speed	m/sec
$C_{1,2,3,4}$	Coefficients	
C_d	Drag coefficient	
C_t	Transport concentration	-
C_v	Volumetric concentration	-
C_x	Drag coefficient	
d	Grain diameter	m
D	Impeller diameter	m

D	Pipe diameter	m
Fr	Froude number	-
g	Gravitational constant	m/sec^2
H	Height	m
I	Mass moment of inertia	$ton \cdot m^3$
k	Constant	-
K_p	Proportionality constant	kNms/rad
L	Length of pipeline	m
n	Revolutions	rpm
p	Pressure	kPa
P	Power	kW
Q	Flow	m^3/sec
r	Radius	m
Re	Reynolds number	-
T	Torque	kNm
u	Tangetial velocity	m/sec
v	Settling velocity grains	m/sec
α,β	Coefficients	
β	Blade angle	rad
ε	Wall roughness	m
ε	Ratio	-
Φ	Durand coefficient	-
η	Efficiency	-
φ	Rotation angle of centrifugal pump	rad
$\dot{\varphi}$	Angular velocity of centrifugal pump	rad/sec
$\ddot{\varphi}$	Angular acceleration of centrifugal pump	rad/sec^2
λ	Friction coefficient	-
ν	Kinematic viscosity	m^2/sec
ρ	Density	ton/m^3
τ	Time constant	sec
ξ	Friction coefficient	-
ψ	Shape factor	

INDICES.

c	Concentration
cr	Critical
c.p.	Centrifugal pump
d	Design
d.e.	Diesel engine
d.f.	Dry friction
D	Diameter

f	Fluid
g	Geodetic
gr	Grain
g.b.	Gear box
h.f.	Hydraulic friction
h.i.	Hydraulic impact
h.p.	Hydraulic power
h.t.	Hydraulic transport
i	In
m	Mixture
m	Measured
n	Revolutions
o	Out
p	Proportional
p	Pump
p	Pipe
q	Quarts
s.p.	Set point
t.	Total
w	Water
0	Initial value (boundary condition)
n	Number of time step
E	Euler
15	%
50	%
85	%